

THE PRESENT DEVELOPMENT OF CSI RICH DETECTORS FOR THE ALICE EXPERIMENT AT CERN

THE ALICE-HMPID GROUP

E. NAPPI, N. COLONNA, D. DI BARI, D. ELIA, R. FINI, L. GALANTUCCI, B.
GHIDINI, A. GRIMALDI, E. MONNO, F. POSA, G. TOMASICCHIO
INFN, Sez. Bari, Bari, Italy

F. PIUZ, A. BRAEM, M. DAVENPORT, A. DI MAURO, D. FRAISSARD, B.
GORET, P. MARTINENGO, G. PAIC, J. RAYNAUD, J. C. SANTIARD, S.
STUCCHI, T. D. WILLIAMS
CERN, Switzerland

Presented by E. Nappi

The ALICE collaboration plans to implement a 12 m^2 array consisting of seven proximity focused C_6F_{14} liquid radiator RICH modules for pion and kaon identification in the momentum range: $1\text{ GeV}/c - 2.7\text{ GeV}/c$.

A large area CsI-RICH prototype has been designed and built to validate the detector parameter assumptions made to predict the High Momentum Particle Identification system (HMPID) performance. The main elements of the prototype will be described with emphasis on the engineering solutions. First results from the analysis of multitrack events recorded with this prototype exposed to hadron beams at CERN SPS will be discussed.

1 Introduction

The experimental programme of the future collider at CERN, the Large Hadron Collider (LHC), includes studies of strongly interacting matter at very high energy densities and temperatures with the aim to reveal fundamental insights into the structure of the QCD vacuum and to give evidence of the phase transition of nuclear matter into the quark-gluon plasma.

Such an opportunity will be exploited by operating LHC with Pb nuclei at a centre-of-mass energy of $2.75\text{ TeV}/\text{nucleon}$ with a luminosity of $10^{27}\text{ cm}^{-2}\text{s}^{-1}$. The challenge of handling the huge multiplicity arising from head-on Pb-Pb collisions and the need to cover the full range of possible signatures, together with a global survey of the events have guided the community of heavy-ion physicists to propose a dedicated experiment that has been approved, under the name ALICE (A Large Ion Collider Experiment), by the LHC Committee (LHCC) to be ready for operation at the startup of LHC. A detailed description of ALICE can be found in ref.¹.

From the artist view of the lay-out, shown in Fig. 1, one immediately recognizes that ALICE consists of two main components: a 2π barrel detector system at

midrapidity embedded within the solenoidal magnet hitherto used in LEP's L3 experiment and a forward muon spectrometer. The following detectors, starting from the beam axis, are sheathed in the L3

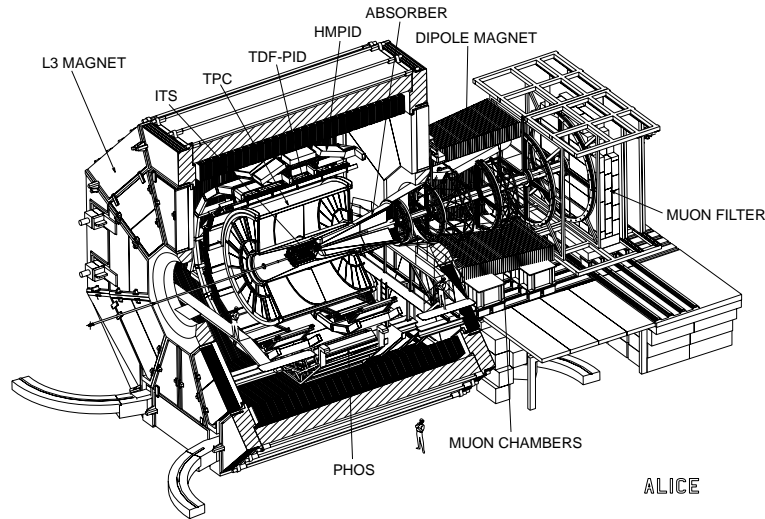


Figure 1: General view of the ALICE lay-out.

magnet:

- an inner tracking system (ITS) with six cylindrical layers of highly accurate position-sensitive silicon detectors;
- a cylindrical, large volume, time projection chamber (TPC);
- a large area particle identification array of time of flight detectors (TOF);
- a second particle identification device for higher momentum particles (HMPID);
- a single arm outer electromagnetic calorimetric complex (PHOS) located below the central barrel region.

A zero degree calorimeter, positioned far downstream in the tunnel, completes the set-up.

Particle identification (PID) in the full range of momentum is crucial for the physics that ALICE is designed to study, indeed TOF and HMPID systems enhance PID capability in the momentum range covered by dE/dx measurements in ITS and TPC and allow to identify particles at much higher momenta than using dE/dx alone.

Namely, the TOF barrel is being optimized for the identification, on a track-

by-track basis, of hadrons with a transverse momentum below 2 GeV/c, with a separation between pions and kaons better than 3 sigmas while HMPID is being designed to extend the useful range to 2.7 GeV/c.

An array of Parallel Plate Chambers (PPC) is the current solution for the low momentum PID system while the Ring Imaging Cherenkov (RICH) technique is the preferred option for the HMPID.

In this paper, the operating principle, the construction and subsequent tests of a large area CsI RICH prototype with features envisioned for the final HMPID module are discussed.

2 HMPID overview

Physics motivations for the single arm HMPID detector are the determination of inclusive particle ratios and transverse momentum spectra in the dense region of the mini-jets that dominate the pre-equilibrium stage of the nucleus-nucleus collisions. Therefore, the HMPID is expected to provide useful information on jet quenching by measuring the ratio of high p_t proton/antiproton spectra. In addition, detector specifications must allow to extend p_t range where Bose-Einstein interferometry with kaon pairs can be studied.

2.1 HMPID design requirements

The design of the HMPID has been governed by the need to cover an hadron identification range from 1 GeV/c to the largest possible momentum by optimizing the detector features mainly on the performance side rather than on efficiency and geometrical acceptance since it will be dedicated only to inclusive measurements.

The particle identification above 2 GeV/c is a challenging task for the TOF technique, whereas an approach based on the detection of Cherenkov light is preferred for the more favourable performance over cost effectiveness ratio. Accordingly, some years ago, the use of a TMAE RICH detector was proposed by some of us². In the meanwhile, several groups actively investigated the opportunity to implement a thin layer of CsI as solid reflective photoconverter in gas counters at atmospheric pressure³, as firstly shown by J. Seguinot et al.⁴. The invaluable advantage of operating the detector at room temperature, without the hazardous photosensitive vapour of TMAE, made the CsI RICH technique a more appealing choice not only for ALICE-HMPID but also for other experiments⁵. Indeed, the risk related to an untested design has been compensated by the simpler construction of the CsI based photodetector geometry and the safer operation over long periods than the TMAE RICH one,

as described onwards.

2.2 Description of the CsI RICH detector

The schematic view of the RICH detector is shown in Fig. 2. The radiator

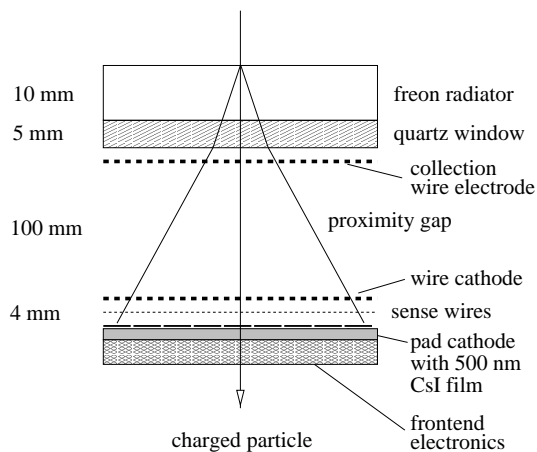


Figure 2: Schematic layout of the fast CsI-RICH.

is a 1 cm thick layer of low chromaticity C_6F_{14} (perfluorohexane) liquid with an index of refraction of $n=1.2834$ at $\lambda=175$ nm corresponding to $\beta_{min}=0.78$ (i.e. a threshold momentum $p_{th}(GeV/c)=1.26 m$, with $m =$ particle mass in (GeV/c^2)).

The photodetector is a multiwire proportional chamber (MWPC), with anode wires of $20 \mu\text{m}$ diameter, 4 mm pitch and 2 mm anode-cathode gap. The MWPC is filled with pure methane at ambience temperature and pressure.

The UV photon conversion into electrons is achieved with a solid photocathode consisting of a thin layer of CsI evaporated onto a plane segmented into pads of almost $8 \times 8 \text{ mm}^2$.

The detector volume, placed in between the radiator and the MWPC, is known as "proximity gap" and is necessary to enlarge the Cherenkov cone to a more convenient size for the imaging. Electrons released by ionizing particles in the proximity gap are prevented to enter the MWPC volume by a positive polarization of the electrode close to the radiator.

A low noise and highly multiplexed VLSI analog electronics is fully integrated

on the back side of the cathode plane, enabling the determination of the hit coordinates by centroid measurements.

The adopted geometry shows the following advantages:

- 1) improved Cherenkov angle resolution since photoconversion is achieved in a single layer without parallax error;
- 2) simplified structure due to the suppression of the photon detector window employed in the case of a TMAE RICH and consequently a cost-saving and a reduced total radiation length;
- 4) mechanical tolerances readily achievable on a large detector surface;
- 5) thin anode-cathode gap (4 mm) which simplifies the cumbersome Cherenkov pattern recognition in high multiplicity environment because the chamber geometry approaches the ideal 2-D geometry and, furthermore it reduces the background since ionizing particles traverse a small sensitive volume;
- 6) short photoelectron collection time that allows operation at high rates;
- 7) an additional tracking plane with good position resolution and multitrack resolution capabilities⁶.

3 Construction details and assembly

The following criteria draw the HMPID engineering design:

- a) a modular construction with elements whose size has been kept as large as technical constraints allow with the aim to keep low the total number needed to cover about 5% of the available phase space in the L3 magnet;
- b) single module orientation in such a way to optimize the Cherenkov angle resolution by minimizing the dip angle of incoming particles;
- c) a cost effective production of system elements with standard techniques where reliability and durability are key factors.

As outcome, the HMPID array consists of seven RICH modules arranged in a barrel section where each module is located on a spherical surface for better incident angles (Fig. 3).

In fact, since the proposed RICH configuration is of a proximity focusing type, it is mandatory that particles impinge on the Cherenkov radiator within a cone of 10^0 around the perpendicular.

The HMPID is at 4.7 m from the interaction vertex, at this distance the particle density is about 50 particles/m², accordingly the pattern recognition is a more feasible task.

3.1 The photodetector

A conventional MWPC, with an active volume of 4 mm depth, 1300 mm width and 1350 mm nominal length, is employed to detect the photoelectrons created

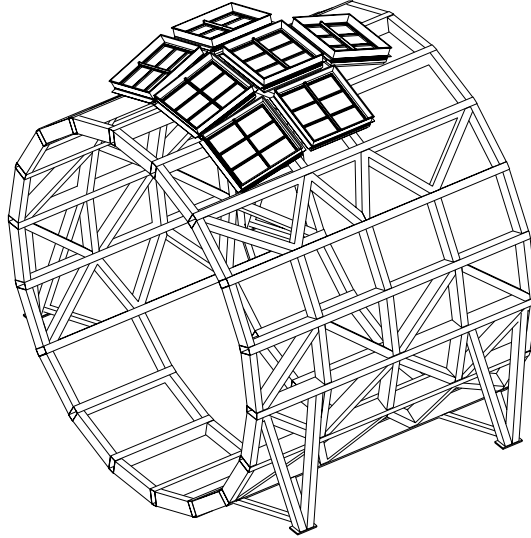


Figure 3: Perspective view of the HMPID layout with the seven RICH modules tilted according to their position with respect to the interaction vertex. The frame that supports the detectors is also shown.

by the photoconversion of Cherenkov photons on the CsI plane and charged tracks with good spatial resolution and high multihit recognition efficiency. The methane gas volume is closed on one side by an end-flange where 6 independent CsI photocathode boards of size $64 \times 40 \text{ cm}^2$ are installed and on the opposite side by a honeycomb panel that supports three C_6F_{14} radiator vessels placed at a distance of 98 mm from the anode wire plane (proximity gap). The anode plane is made of 300 gold plated tungsten wires, spaced 4 mm apart. The anode-cathode gap is 2 mm. The $20 \mu\text{m}$ thick anode wires are soldered on a G-10 printed board with a precision of 0.1 mm and a tension of 50 g. On both the edges of the anode plane, thicker guard wires are installed to resist the boundary discontinuity of the electrostatic field. The wire gravitational sag is reduced by one precise MACROLON spacer glued onto the central part of the anode plane (Fig. 4). The second cathode plane is built out of $50 \mu\text{m}$ diameter wires. A positive voltage of 2100 V applied to the anodes, while cathodes are grounded, provides a total gas gain of almost 10^5 .

A relevant feature of the adopted design for the HMPID photodetector is

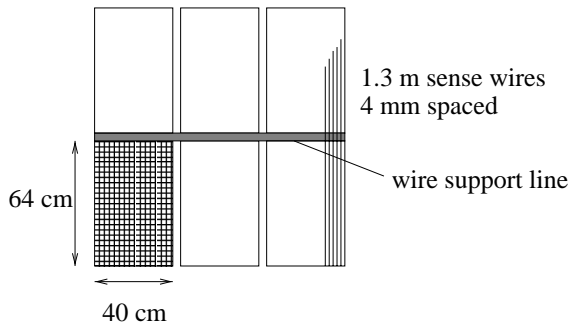


Figure 4: Top view of the photodetector anode plane with the wire support spacer. One CsI board, out of six forming the pad cathode plane, is also shown.

the "open geometry" i.e. the suppression of electrode elements that in TMAE photodetectors are specifically implemented to prevent spurious avalanches from feedback photons. In fact, as it will be reported in the next section, the expected negligible background level does not require any complex blinding structure.

An aluminum alloy has been carefully selected as frame material to minimize outgassing into the chamber active volume. The gas tightness is ensured by soft O-rings placed in grooves in the chamber frames. Four gas inlets and outlets provide an uniform gas flow, at a pressure slightly above 1 bar, of 40 l/h. With this flow rate, the volume of each HMPID module is completely refreshed every 4 hours. Typical O_2 and H_2O content, monitored at the outlet, is of 5-8 ppm.

3.2 The CsI photocathode

A specific R&D for the development of CsI photocathodes of large area was approved in 1992 by the DRDC at CERN under the name RD26⁷.

RD26 achieved a break-through in CsI deposition techniques by developing a successful standardized technology of evaporating photocathodes, as large as $50 \times 50 \text{ cm}^2$, without the expensive and time-consuming implementation of masking techniques⁸.

The pad cathode is built according to the criteria of having a stiff and flat plane made out of light materials (less than 0.01 % X_0). The proposed solution is

a 40 mm thick slab of ROHACELL (density 30 g/l) sandwiched between two 0.8 mm thin foils of copper printed circuit boards.

The best CsI quantum efficiency (QE) is obtained by depositing at least 250 nm of CsI onto a printed circuit boards with a copper layer, accurately pre-polished through mechanical and chemical treatments, subsequently covered with a thick (7 μm) chemically deposited nickel layer followed by a thinner (0.5 μm) layer of gold⁹.

The photocathodes are prepared in a large evaporation stand, placed at CERN, equipped with four DC heated tungsten crucibles operated simultaneously to achieve an uniform CsI layer. During the deposition, the pad substrate is held at 50 $^{\circ}\text{C}$. A 12 hours post-deposition heat treatment at 60 $^{\circ}\text{C}$, under vacuum, is necessary to achieve the final CsI QE¹⁰.

The installation of the photocathode boards in the MWPC is carefully performed by using a large volume glove box, flushed with Argon, that avoids any direct contact of the photosensitive film with air, in fact it is well known that although short exposures to air may be tolerable, the presence of water vapour produces unrecoverable loss in CsI QE⁹.

3.3 *The liquid radiator vessel*

The C_6F_{14} radiator vessel represents a critical part in the detector design. The rather high perfluorohexane and silica glass densities, 1.68 g/cm³ and 2.1 g/cm³ respectively, and the need to avoid pollution from the material in contact with the liquid radiator that would affect the transparency in the 160÷220 nm band, required a careful investigation and optimization.

The liquid radiator container, which is currently under study, consists of a tray made of NEOCERAM closed by a UV-grade fused silica plate. Their thickness and size have been carefully optimized by investigating the best compromise between the detector total radiation length and the perfluorohexane hydrostatic pressure, in the current geometry the quartz window is 5 mm thick, while the NEOCERAM base plate is 4 mm thick. Moreover, given the quantum efficiency achieved so far, the radiator thickness is chosen 10 mm for an optimal Cherenkov angle resolution.

NEOCERAM is a glass-ceramic material, thermally compatible with the fused silica (thermal coefficient $0.5 \cdot 10^{-6} \text{ }^{\circ}\text{C}^{-1}$). The vessel elements are glued together with Araldite AW106. The liquid radiator inlet and outlet are obtained by inserting two stainless steel pipes on the opposite edges of the NEOCERAM tray, the outlet always being at the highest location.

To withstand the hydrostatic pressure, eighteen cylindrical spacers are glued

to the NEOCERAM bottom plate on one side and the quartz window on the other side. Spacers consist of fused silica rods with a diameter of 10 mm placed in two rows of 9 equi-spaced elements.

Each HMPID module has three independent radiator trays of $1330 \times 413 \text{ mm}^2$, supported by a stiff composite panel made out by sandwiching 50 mm of an aramide-fibre epoxy honeycomb material between two 0.5 mm thin layers of aluminum (Fig. 5). The HMPID geometrical acceptance is determined by the

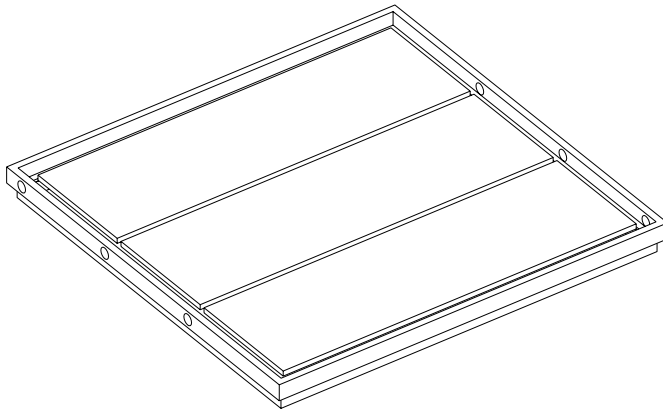


Figure 5: Perspective view of the HMPID honeycomb panel with the three radiator vessels.

modular structure of the detector and by the modularity of the quartz windows, it is about 70% in the present engineering design.

The radiator vessel and the contained fluid dominate the bulk of the detector material, estimated to be 16% X_0 (table 1). A full scale vessel prototype has been realized to prove the mechanical viability of the adopted solution. Strains and deflections of the vessel elements have been measured by strain gauges during tests in several hydrostatic conditions.

3.4 The readout electronics

Considering the large number of channels in use ($\simeq 16000$ per m^2), a dedicated electronics has been developed to better exploit the potentialities of the

Table 1: Mass composition of the HMPID module

<i>Material</i>	<i>Thickness(mm)</i>	<i>X/X₀</i>
<i>Honeycomb back panel</i>	50	0.02
<i>Neoceram plate</i>	4	0.03
<i>Quartz window</i>	5	0.04
<i>C₆F₁₄</i>	10	0.05
<i>Photocathode plane and electronics</i>	1	0.02

Table 2: Specifications of the 0.7 μm version of the GASSIPLEX chip

<i>Noise(r.m.s.)</i>	650 <i>e</i> at 0 <i>pF</i>
<i>Noise slope</i>	< 11 <i>e r.m.s./pF</i>
<i>Min – max input sensitivity</i>	4-10 <i>mV/fC</i>
<i>Baseline recovery</i>	< 0.5% after 6 μs
<i>Peaking time</i>	1.1 – 1.3 μs
<i>Power consumption</i>	< 8 <i>mW/ch</i>
<i>Analog read – out speed</i>	10 <i>MHz</i>

CsI-RICH technique with cost effectiveness in mind.

A favourable factor is the low interaction rate expected when LHC is operated with lead ions at the luminosity of $2 \cdot 10^{27} \text{ cm}^{-2}\text{s}^{-1}$. The interaction rate will likely reach about 10^4 Hz for minimum bias collisions, a small fraction of which, approximately $2 \div 3\%$, corresponds to the most interesting central collisions with maximum particle production. Consequently, the number of digital elements can be reduced by using a certain level of multiplexing in the analog signal processing.

A VLSI front-end chip, referred as GASSIPLEX, based on a 16 channels analog multiplexed scheme operated in Track and Hold (T/H) mode has been designed. A specific filter, that takes into account the MWPC input current shape, performs a base line restoration at 0.5% of the peak amplitude in less than 6 μs . The signal of the shaping stage peaks at 1.2 μs corresponding to the latency of the zero level trigger that sends the T/H signal. The performances of the GASSIPLEX are summarized in table 2.

The read-out architecture is organized as a Multi Chip Module (MCM)¹¹ com-

posed of 4 "daisy chained" GASSIPLEX's followed by a single 10 bit-ADC and a logic C-MOS chip, referred as DILOGIC, performing the necessary zero suppression for sparse read-out. The full processing time of the 64 channels of a MCM takes $8 \mu\text{s}$ to provide digitized data, amplitudes and addresses, stored in a FIFO memory ready to be transported via optical link to the central data recording system.

The electronics is uniformly distributed on the back side of the cathode pad plane. Electrical connections are achieved through Kapton buses which are directly soldered on the ends of the traces that carry signals from the pads to the MCM board. (Fig. 6).

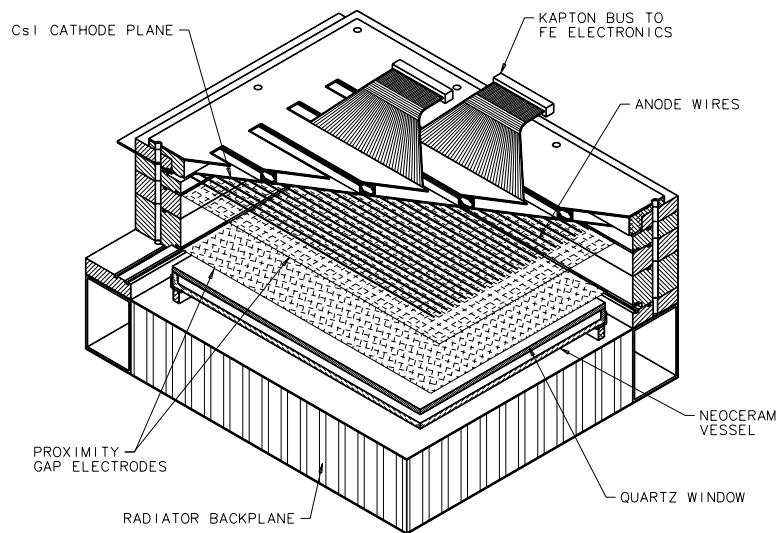


Figure 6: Cut away view of the HMPID CsI-RICH showing separately each detector component. Kapton buses that carry signals from the pads to the readout electronics are also shown.

4 PS and SPS beam test results

During the past three years, the performance of 32 large size photocathodes has been evaluated by exposing them to various test beams at CERN-PS(T11) and SPS(H4). PCs of size $30 \times 30 \text{ cm}^2$ have been tested using our first Fast-RICH prototype¹² while the PCs of final HMPID size ($64 \times 40 \text{ cm}^2$) have been installed on a larger RICH prototype representing 2/3 of the ALICE module.

Small photocathodes, as well as full HMPID size one, have been used with C_6F_{14} .

The sensitivity of the current FE electronics (GASSIPLEX) allows to operate the photodetector at a total gain lower than $2 \cdot 10^5$, with a mean noise performance of 1200 electrons r.m.s. for 13000 channels. The chamber is operated in a proportional mode showing a pure exponential shape for the pulse height distribution obtained with single electrons¹². A 3σ threshold corresponds to a 95% efficiency for detecting single electrons.

The exposure to minimum ionizing particles (MIP), at 10 kHz rate, causes a current of less than 6 nA at $2 \cdot 10^5$ gain, due to both particle and Cherenkov photoelectron ionisations into the MWPC gap. Under these conditions, the detector has demonstrated a very stable operation over test periods of months, with practically no instabilities such as micro discharges. The levels of oxygen and water vapor in the operating gas, CH_4 , have been kept below 50 ppm and 8 ppm in the small and large prototypes, respectively.

The main features in detecting Cherenkov rings from pions of high beta (PS beam at 3 GeV/c and SPS beam at 350 GeV/c) at normal incidence using a 10 mm thick C_6F_{14} radiator are the following:

- 1) an average number of 16 photoelectrons per ring (Fig. 7a);
- 2) an angular resolution of 7.4 mrad per photon (Fig. 7b);
- 3) an average background due to photon feedback (essentially generated by the charged track avalanches) that increases with the chamber gain and is lim-

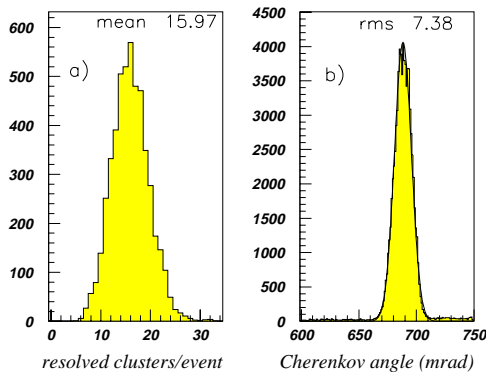


Figure 7: a) number of resolved photoelectrons per event, b) reconstructed Cherenkov angle per photon.

ited at the highest gain to about 1.5 hit per ring found outside the fiducial

Cherenkov area.

Photocathode performances have been steadily reproduced for each of the 13 PC's where the substrate and CsI layer processings were implemented according to the treatment described in Section 3.2. Moreover the photocathode behaviour has been found stable over 2 years: when not used, CsI-PC's were kept under constant protection with an argon flow.

Furthermore a detector with a CsI photocathode total area of 0.4 m² has been used in a lead ion run as a Threshold Imaging Cherenkov detector by the NA44 collaboration with satisfactory results¹³.

In parallel to the PS tests, an extensive ongoing investigation on a 130x80 cm² prototype has been undertaken to validate the engineering design adopted and to study pattern recognition issues under expected background conditions.

An initial period of test with the 340 GeV/c pion beam at CERN-SPS has been performed for three consecutive weeks in September and October 1997.

A system for the circulation and purification of C₆F₁₄ that includes monitoring and control features has been specifically built.

Fig. 8 shows the perfluorohexane transmission in the UV region before and after purification by passage through a molecular sieve. C₆F₁₄ was provided by the PERFORMANCE FLUID Division of 3M Corporation, item PF-5060. During the run period, the levels of oxygen and water vapour in the gas volume

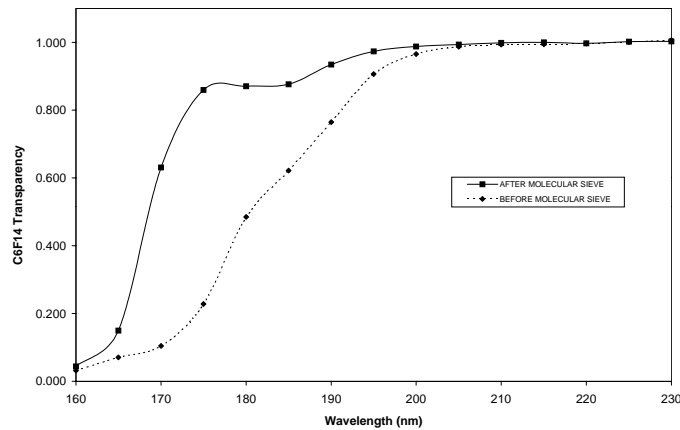


Figure 8: C₆F₁₄ transmission plots before and after the molecular sieve purification.

were always below 20 ppm and 3 ppm respectively due to the very low out-

gassing rate of the prototype.

A telescope of three multiwire chambers measured the direction of each incident particle. Scintillator counters defined the beam and the trigger.

The system has worked flawlessly without any intervention. Data were collected at different particle densities from few particles per m^2 to more than 50 particles per m^2 . A fully reconstructed SPS event is shown in (Fig. 9), the analysis of the entire data set is in progress.

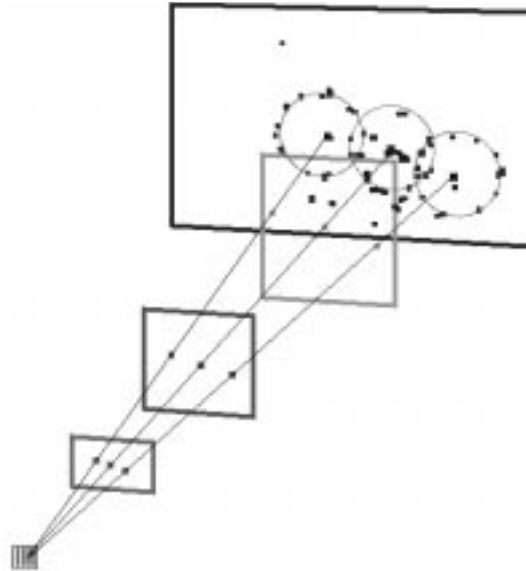


Figure 9: Display plot showing an SPS event. Three tracks are reconstructed by using the tracking chamber telescope, the associated rings are shown in the HMPID prototype.

5 Particle identification capability

The most serious challenge to the HMPID performance is the pattern recognition in the presence of a large number of photons. A full GEANT simulation of LHC events at the position of the HMPID that takes into account the secondary particles produced in the HMPID itself has been developed to assess the pattern recognition capabilities. The simulation of the MWPC response has been based on experimental data acquired with prototypes using minimum ionizing particles and single photoelectrons.

A reconstruction method based on a one-dimensional “Hough-like” transform that maps the pad coordinate space directly to the Cherenkov angle parameter space has been applied to analyse the simulated events¹⁴.

The results indicate that a satisfactory PID may be achieved for densities up to 50 particles/m² at the quantum efficiencies presently obtained on large photocathodes: 3σ π /K separation at 2.7 GeV/c¹.

A test with very high particle density is planned by November 1998 with heavy ion beams at CERN-SPS. It will represent the ultimate test of feasibility for the RICH concept in HMPID.

6 Conclusions

ALICE is a 4π detector with emphasis on particle identification, high granularity and precise impact point localization. To meet the requirements for particle identification in the region above 1 GeV/c, an approach based on the RICH technique with photodetectors having a true bi-dimensional readout has been proposed and investigated.

The proposed modular design should allow a simple and cost effective scheme, consisting of a classical MWPC operated at normal temperature and pressure, and of a liquid radiator (C_6F_{14}).

Pattern recognition can be successfully implemented on high density events (50 tracks per m²), since an analog pad read-out scheme provides efficient discrimination between ionizing particle and Cherenkov photoelectron signals. Conceptual engineering studies have been carried out for the base module and the mechanical viability of the chosen solution has been demonstrated on large scale prototypes.

Although the application of CsI in large area Cherenkov counters is a new development with unexplored risks associated with the manufacture, handling during assembly and maintenance during operation, extensive beam tests with a realistic mechanical layout proved that all components function reliably.

Acknowledgements

We are grateful to L. Dell’Olio, D. Dell’Olio, N. Facchini, E. Gaumann, L. Liberti and V. Valentino for their competent and continuous support on the development of the NEOCERAM vessel.

References

1. ALICE Technical Proposal, CERN/LHCC 95-71.
2. E. Nappi et al., Nucl. Instr. and Meth. A315(1992) 113.
3. Proceedings of the 2nd Workshop on Ring Imaging Cherenkov Detectors (RICH95) Nucl. Instr. and Meth. A371(1996), Section III.
4. J. Seguinot et al., Nucl. Instr. and Meth. A297(1990) 133.
5. HADES, Proposal for a High Acceptance Di-Electron Spectrometer, GSI/Darmstadt (1993); COMPASS, Proposal, CERN SPSCL/96-14,SPSCL/P297.
6. D. Di Bari et al., ALICE Internal note ALICE/97-39.
7. E. Nappi et al., RD26 proposal to DRDC, CERN/DRDC 92-3 and ADDENDUM to the DRDC PROPOSAL P35, CERN/DRDC/92-16.
8. RD26 status report, CERN/LHCC 96-20.
9. F. Piuz, Nucl. Instr. and Meth. A371(1996)96.
10. A. Buzulutskov et al., Nucl. Instr. and Meth. A366(1995) 410.
11. J.C. Santiard, A compact on-detector analog to digital processor, CERN/ECP/MIC, 1996.
12. A. Braem et al., Nucl. Instr. and Meth. A343(1994) 163.
13. S. Esumi et al.,Fizika B4(1995)205 and A. Braem et al., CERN/PPE-97/120.
14. A. Di Mauro et al., Nucl. Instr. and Meth. A343(1994) 284.